

# Design- and Simulation-based Comparison of Grid-Forming Converter Control Concepts

Christian Schöll, Hendrik Lens

University of Stuttgart, IFK

Pfaffenwaldring 23, 70569 Stuttgart, Germany

Email: {christian.schoell;hendrik.lens}@ifk.uni-stuttgart.de

**Abstract**—Until now, the textbook example of voltage source behavior along with the provision of inertia is the behavior of the synchronous generator (SG). This can be explained by the historical success of large scale electrification with AC power systems, which is closely linked to the SG. Therefore, previously SG-based electrical power systems face significant challenges due to the shift towards renewable energy sources (RES). Being generally converter-based, these do not provide essential stabilizing properties as SG do. Consequently, beyond a certain share of this kind of generation, interconnected power system stability is at stake. If, on the other hand, the previous paradigm of converter control is changed, then system operation without any SG is possible. To this end, the converters have to exhibit essential voltage source properties as SG do. Such converters are then referred to as grid-forming converters (GFC). However, the dynamic behavior of GFC is not defined by physical properties as in the case of SG. It is defined by the grid-forming control concept only, providing a high degree of freedom for possible implementations. Taking advantage of this freedom, a wide range of different, but partly also similar or even equivalent grid-forming control concepts have been developed in recent years. Therefore, in this paper, ten of today's most discussed control concepts are compared. In this comparison, unique features, similarities and equivalences of the control concepts are shown. The focus is on the instantaneous and stationary behavior of the control concepts, which is analysed by means of a system-theoretical and simulative analysis. The insights gained from this comparison can be helpful for the functional specification, development and improvement of GFC, as the variety of control concepts can be better understood.

## I. INTRODUCTION

Inertia and voltage source behavior are essential for the stability of interconnected power systems. At present, these essential properties are provided by synchronous generators (SG) of conventional and hydro power plants. Aiming at a zero carbon energy system, more and more conventional power plants are mothballed. Consequently, the share in power generation of SG, which intrinsically provide these essential properties, is decreasing, causing stability reserves of the power system to decline.

A widely discussed possible solution to overcome this problem are grid-forming converters (GFC). GFC generate a voltage, adjusting the set-points for the voltage phase angle and amplitude according to a given control concept without controlling the resulting currents directly as long as they remain in the admissible range. The currents adapt to the needs of the grid, so that an intrinsic contribution to power system stability similar, albeit not identical, to the contribution of SG can be achieved.

While the dynamic behavior of a SG is defined by its physical properties, the dynamic behavior of a GFC

only depends on its control concept, opening a wide range of possible implementations. Although these concepts are mainly based on the same fundamental principle of power synchronization as SG, there are differences in their dynamic behavior and the way how synchronization with the grid is achieved. Some of the GFC control concepts discussed for the use in interconnected power systems originally have been developed for microgrid applications. Furthermore, existing developments have been modified and adapted to address the needs of interconnected power systems, ultimately resulting in a wide range of concepts that are currently under discussion.

Several existing publications aim at comparing GFC control concepts. A general overview of the most frequently discussed control concepts is given in [1]. Equivalences and similarities between the concepts are specifically pointed out using appropriate transformations of the system equations and block diagrams. In [2] and [3], selected concepts are compared in detail. Differences in their dynamic behavior are investigated by means of simulations, but only a smaller number of the relevant concepts are used for these comparisons.

Thus, the goal of this paper is to compare a large number of today's relevant control concepts by 1) a detailed system-theoretical analysis of their design and by 2) a comparison of their dynamical behavior in simulation-based studies. The control concepts are compared with respect to their instantaneous and stationary response to phase jumps and to frequency changes during normal operation. Concepts to maintain the current within the hardware capabilities during severe events are not considered.

For the purpose of comparison, the simulation models of the various control concepts are configured such that they provide comparable changes in active power for a given phase jump and for a given Rate of Change of Frequency  $\dot{f}$  (RoCoF), respectively. Thus, differences in their dynamic behavior become apparent as well as whether an active power component is provided that is directly proportional to the frequency deviation.

In the following chapter, first the fundamental design features of GFC control concepts are introduced. Subsequently, the control concepts are presented as they can be found in the literature. Distinctive characteristics and special features with regard to their dynamic behavior are highlighted. Possible modifications of one of the most widespread GFC control concepts, the Swing Equation, are presented. After the presentation of all GFC control concepts, they are then compared in terms of their system-theoretic representations

and finally in terms of simulations.

## II. GRID-FORMING CONVERTER CONTROL CONCEPTS

A generally applicable definition or regulatory requirement for the behavior of GFC is not available yet. However, [4] compiles fundamental requirements for GFC without specifying any concrete implementation details. Based on this, [5] and [6] further substantiates these essential properties with respect to future energy systems without SG. Accordingly, an essential feature of GFC is a voltage source behavior together with the provision of inertia. Whereas [5] is focused on testing of low voltage converters up to several MW, [6] is focused on high-voltage direct current (HVDC) systems, based on simulation. This fundamental paradigm for the control of GFC already defines the basic control design principles for their dynamic behavior.

Conventional, so called grid-following converter control concepts, i.e. current control in  $dq$ -coordinates [7], result in a current source behavior of the feed-in. The operation of grid-following converters requires the point of connection to be characterised by a sufficiently stiff grid voltage. Grid-forming control concepts pursue the objective of letting the converter behave as a voltage source. This generally excludes fast control of the resulting converter currents. In fact, the output currents should be able to react freely according to the needs of the grid within the technical limits of the converter. Accordingly, a GFC has to adjust its output voltage phasor after a change of the grid voltage phasor in such a delayed way that a voltage source behavior is maintained. Analogously to SG, this implies that the converter phase angle and the voltage amplitude may not change in a stepwise fashion. On the contrary, they have to counteract transient changes in the grid by equipping the voltage phasor with inertia.

Although grid-forming and grid-following control concepts are based on the same inputs, i.e. active power difference  $\Delta p$  and reactive power difference  $\Delta q$ , a GFC control concept does not generate current setpoints but rather phase angle  $\theta$  and voltage amplitude  $\hat{u}$  setpoints to be realized by the converter. The dynamics between these input and output variables are in the hands of the control engineer. In this respect, the focus of this paper is on active power behavior. Therefore, only the active power parts of the grid-forming control concepts providing the phase angle setpoint  $\theta$  are presented. The corresponding reactive power parts, which provide  $\hat{u}$ , mostly have a similar structure and can be taken from the given references.

The considerations in this paper are therefore based on the assumption that  $p$  and  $q$  can be controlled separately. This assumption is valid in predominantly inductive networks, i.e. those in which the reactance of the lines is greater than the active resistance.

### A. Swing Equation (SE)

A widespread option for power synchronisation is to mimic the dynamics of a SG, which is well-known as *virtual synchronous machine* (VSM) [8]. Fig. 1(a) shows a possible active power part of a VSM based on the well-known second order swing equation. Analogously to SG, a difference in active power  $\Delta p$  calculated as the difference between the

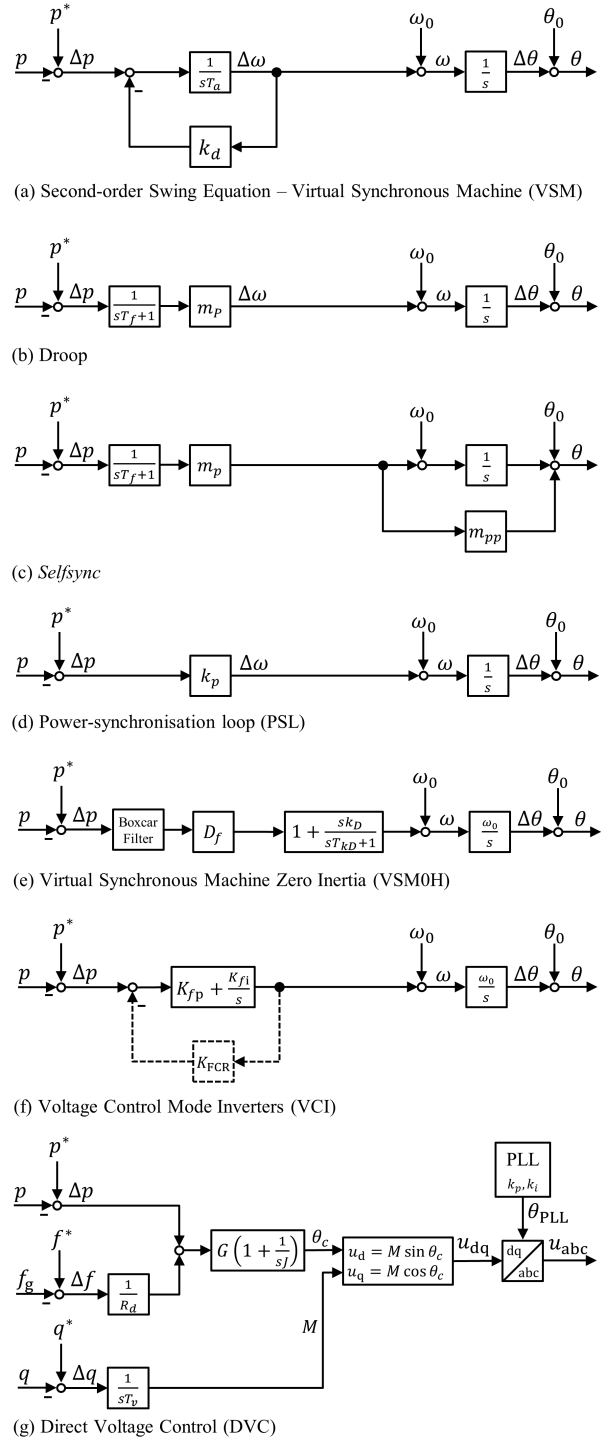


Fig. 1. Overview of the grid-forming converter control concepts. The control concepts are largely illustrated as they can be found in the literature.

setpoint value of the active power  $p^*$  subtracted from the actual value of the active power output  $p$  is interpreted as the angular acceleration  $\ddot{\theta}$  of a virtual flywheel, characterized by  $T_a$  analogous to the acceleration time constant of SG. Additional damping is achieved by means of a frequency droop characterized by  $k_d$  based on the frequency deviation  $\Delta\omega$ . Such a damping term differs from the behavior of a real SG in the sense that it corresponds to instantaneous provision of frequency containment reserve (FCR). Real SG that provide FCR need a change of the mechanical power to

do so, which cannot take place instantaneously due to the dynamics of the process that drives the turbine. This is an important difference between VSM and SG. The converter frequency  $\omega$  is calculated by one-time integration of  $\dot{\theta}$  along with the nominal frequency  $\omega_0$ . Further integration with the addition of the initial value of the phase angle  $\theta_0$  results in the output phase angle  $\theta$ . From this it can be concluded that both converter frequency and phase angle cannot change in a stepwise fashion.

### B. Droop

The grid-forming control concept *droop*, which originates from microgrid control, pursues the goal of interpreting the active power difference  $\Delta p$  as a converter frequency setpoint by means of a droop factor  $m_p$ . As shown in Fig. 1(b), the active power difference is delayed by means of a first order linear time-invariant (LTI) system characterized by the time constant  $T_f$  and is then fed to the droop. Thus, as with the SE, there is no feedthrough between the input  $\Delta p$  and the converter frequency  $\omega$ . It should be noted that the droop concept is equivalent to the SE with regard to dynamics [9]. The parameters can be chosen such that the exact same dynamic behavior can be observed. Due to this equivalence, the control concepts have the same properties in terms of both inertia provision and FCR.

### C. Selfsync

If an additional feed-forward path is implemented along the angular integrator in the droop concept, damping behavior is improved. This control concept, then known as *Selfsync* [10], is shown in Fig. 1(c). While the frequency  $\omega$  of the converter voltage is directly accessible from the droop concept, this is no longer possible with *Selfsync*. Due to the additional phase angle signal characterized by  $m_{pp}$ ,  $\dot{\theta}$  does not correspond to the input of the second integrator. Hence, this extension implies that the converter frequency can change step-wise. Nevertheless, the converter phase angle cannot change in a step-wise fashion.

### D. Power-Synchronisation Loop (PSL)

The control concept Power-Synchronisation Loop (PSL) [11] originates from the control of high-voltage direct current transmission systems. As shown in Fig. 1(d), it represents the control concept with the lowest complexity in this paper. An active power difference is interpreted as the converter frequency, characterized by  $k_p$ . It is immediately visible that this control concept does not provide inertia apart from inevitable small time constants related to the active power measurement. PSL provides an active power proportional to the frequency deviation in the sense of FCR.

### E. Virtual Synchronous Machine Zero Inertia (VSM0H)

According to [12], the Virtual Synchronous Machine Zero Inertia (VSM0H) concept, shown in Fig. 1(e), represents a VSM without any contribution to inertia. And in fact, the control concept does not contain any mechanisms which are intended to purposely introduce inertia. The contribution to inertia due to the adaptive boxcar filter, used as an averaging filter to determine active power, is negligibly small. This results in a strong similarity to the PSL presented above. In

addition to the use of the boxcar filter, however, the VSM0H also has an additional filter to dampen possible resonance phenomena.

### F. Voltage Control Mode Inverters (VCI)

In contrast to the SE, the control concept Voltage Control Mode Inverter (VCI) shown in Fig. 1(f) has a PI system between the active power difference and the converter frequency instead of a single integrator [13]. This additional proportional component indicates that the converter frequency can now perform step changes. Optionally, the authors consider an additional feedback term to provide FCR.

### G. Direct Voltage Control (DVC)

At first glance, the control concept Direct Voltage Control (DVC) [14] in Fig. 1(g) shows significant differences from the other control concepts presented so far. The most significant difference is the use of a phase-locked-loop (PLL) for synchronization with the grid. First, an internal converter angle  $\theta_c$  is generated based on  $\Delta p$  and optionally the grid frequency deviation using a PI system. In combination with the internal voltage amplitude setpoint,  $M$ , based on  $\Delta q$ , the internal converter voltage is then transformed into the  $dq$ -system. Finally, the internal  $dq$  converter voltages are transformed into the three-phase converter voltages  $u_{abc}$  based on the grid voltage phase angle  $\theta_{PLL}$  of the PLL. The dynamic behavior of the converter therefore additionally depends on the dynamics of the PLL. Noticeable in this variant of the DVC is a feedthrough-component between  $\Delta p$  and  $\theta$ . This means that the converter voltage phasor can theoretically perform stepwise changes. This would contradict the basic idea of a GFC. In reality, however, it can be assumed that additional delays in the active power difference would prevent this behavior. Therefore, in our simulation model of the DVC, a first order LTI system for  $p$  with  $\tau = 20$  ms was assumed. Nevertheless, it must be noted that this assumed delay is not a conceptual property. It should also be noted that the authors of [14] intend a current limitation, which temporarily switches to a current-controlled operation based on fault detection. This has no influence on the behavior in normal operation and is therefore not considered in this paper.

## III. MODIFICATIONS OF THE GRID-FORMING CONVERTER CONTROL CONCEPTS

With the aim to obtain better control and damping behavior or to prevent undesired FCR provision, as well as an energy store required for this purpose, various modifications of the control concepts are discussed. In this paper, we focus on three modifications of the SE or its systems theoretically equivalent droop concept, respectively. Note that some of these modifications can be implemented in a similar form with the other grid-forming control concepts.

### A. Swing Equation with Autonomous Frequency (SEAF)

Usually, the control concepts describe the dynamic behavior of the frequency around the nominal frequency  $\omega_0$ . For the SE, droop and other control concepts, this leads to a FCR provision in case of a permanent frequency deviation.

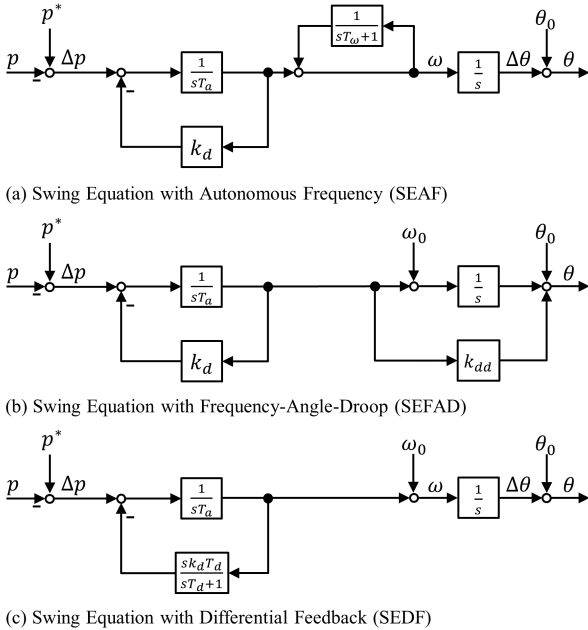


Fig. 2. Modifications of the SE-based VSM concept.

However, in order to maintain sufficient damping, it is not practical to set the feedback term  $k_d$  of the SE to 0. This would lead to undamped behavior of a double integrator. Therefore, the first modification presented in this paper adjusts the internal value for the nominal frequency  $\omega_0$ . This can be achieved by feedback of the converter frequency as shown in Fig. 2(a). The initial dynamic behavior after a step change in  $\Delta p$  is still characterized by  $T_a$ , while the subsequent stationary behavior is characterized by  $k_d$  and  $T_\omega$  of the feedback paths. An alternative to this approach, which is not considered in more detail in this paper, is a lagging of the measured grid frequency. The resulting behavior then differs from the modification shown in Fig. 1(a) due to the influence of the coupling impedance and the characteristic of the frequency measurement.

### B. Swing Equation with Frequency-Angle-Droop (SEFAD)

Analogous to the *Selfsync* concept, a droop between the converter frequency and phase angle leads to an improvement of the damping behavior of the SE [15]. The modified SE concept is shown in Fig. 2(b). This modification of the SE concept now allows to parameterize the feedback term  $k_d$  to 0, thus additionally avoiding FCR provision. However, as with *Selfsync*, this modification implies that the converter frequency can now change step-wise.

### C. Swing Equation with Differential Feedback (SEDF)

Alternatively, the provision of FCR can be avoided by introducing a differential feedback component, as shown in Figure 2(c). Depending on the choice of the time constant  $T_D$ , the damping property of the feedback is maintained for a limited period of time. The instantaneous behavior is still characterized by  $T_a$ , while similar to SEAF, the stationary behavior is additionally characterized by the choice of  $k_d$  and  $T_d$ .

## IV. COMPARISON OF THE CONTROL CONCEPTS

In the previous chapter, major characteristics of the control concepts were highlighted on the basis of their block diagrams. In this chapter, the control concepts are first compared on the basis of their transfer functions and then by means of simulations during frequency changes and phase angle jumps.

### A. Theoretical comparison

Converting the control concepts into their basic mathematical form in terms of transfer functions allows for a straightforward comparison and enables further analyses on their dynamic behavior largely independent of a specific parameterization. For this purpose, the control concepts are shown in Table I together with their associated transfer functions between the input  $\Delta p$  and the output  $\theta$ , provided that the control concept is linear. Note, that the transfer functions are only valid as long as the converter current limit is not reached, as this renders the system behavior nonlinear.

The direct comparison of the transfer functions of the control concepts shows further strong similarities or, with certain parameterizations, even equivalent system representations. Worth being mentioned are, besides the already known equivalence between SE and droop, the similarity between PSL and VSMOH, as well as between *Selfsync*, VCI and SEFAD. Another structural similarity can be observed between SEAF and SEDF.

The comparison is now extended by another characteristic of the control concepts in order to better understand their dynamic behavior. For this purpose, the derived transfer functions are used to characterize the dynamic behavior according to the final value theorem for a step-wise change in  $\Delta p$ .

Here, the focus is on the dynamic behavior of the converter phase angle, with its acceleration behavior being of particular interest. Therefore, the respective two-times differentiated transfer function

$$\frac{\ddot{\theta}(s)}{\Delta p(s)} = s^2 G(s) \quad (1)$$

of each individual control concept is considered. Subsequently, the reciprocal values according to the final value theorem are calculated for two cases. In the first case, the behavior at the beginning of an excitation is calculated according to

$$\lim_{t \rightarrow 0} \frac{\ddot{\theta}(t)}{\Delta p(t)} = \lim_{s \rightarrow \infty} s \frac{\ddot{\theta}(s)}{\Delta p(s)}. \quad (2)$$

In this paper, this relationship is interpreted as the instantaneous behavior of a control concept. Analogously, in the second case the stationary behavior is analyzed according to

$$\lim_{t \rightarrow \infty} \frac{\ddot{\theta}(t)}{\Delta p(t)} = \lim_{s \rightarrow 0} s \frac{\ddot{\theta}(s)}{\Delta p(s)}. \quad (3)$$

The reference of the comparison is the dynamic behavior of the SG. The damping behavior of the SG is contained in  $\Delta p$ , thus, in simplified fashion, there is a double integrator with respect to the input-output behavior.

Under this consideration, both instantaneous and stationary behavior of the SG are exclusively characterized by

its inertia constant  $T_a$ . Based on the underlying physical relationship, this is not surprising. Any change of the rotor angle requires to overcome the inertia of the rotating mass of the SG. A step change of the rotor frequency or even the rotor phase angle is impossible for physical reasons. On the other hand, the grid-forming control concepts developed are not constrained by such fundamental physical relationships. The instantaneous and stationary behavior depend on the implemented control algorithm and the selected parameters.

This can be seen from the control concepts of SE and droop. Their instantaneous behavior is comparable to that of a SG. The acceleration of the converter phase angle  $\dot{\theta}$  is limited by the control concept and cannot perform step changes. If, on the other hand, the acceleration of the phase angle is not limited, the frequency can perform step changes. Based on this consideration, all control concepts that have a 0 in the column *Instantaneous Behavior* of Table I are capable of changing the converter frequency in a stepwise fashion. It is worth noting, that this is true for all control concepts that have a feed-through along an integrator.

The stationary behavior of the SE and droop, on the other hand, is characterized by the provision of FCR intrinsic to this control concept. A network consisting only of feed-ins with this control concept would reach a new steady-state frequency after a load step. Such a system would therefore have a theoretically infinite inertia based on steady state. In contrast, the frequency in a network consisting of uncontrolled SGs would ramp down towards 0 Hz. The slope of the frequency ramp would depend exclusively on the respective inertia constants of the SGs, which is known as inertial response [16]. Thus, in the case of a longer lasting frequency ramp of a SG, a stationary active power output proportional to its inertia constant  $T_a$  and the steepness of the frequency ramp, would occur after a transient settling period. Based on this consideration, all entries in the *Stationary Behavior* column of Table I which are infinite must be considered as FCR provision. A finite value indicates that the behavior is comparable to an uncontrolled SG after finite time.

### B. Simulative comparison

In order to verify the results obtained on the basis of theoretical analyses, the concepts are now compared by means of simulations. The network model used for this purpose is shown in Fig. 3 and consists of a GFC, a SG, a node, and a stiff voltage source of variable frequency and phase angle. The SG and the GFC are connected to the node by means of the same filter reactance  $x = 0.1$  pu. The nominal apparent power of the GFC and the SG is 100 kVA each. SG and GFC are investigated in separate simulations. All simulations were carried out with the simulation software *PowerFactory* in the EMT domain.

In order to analyse the intrinsic, transient, and stationary behavior, the responses to a phase angle jump and a frequency ramp of the voltage source are simulated. First, a phase angle jump of  $1^\circ$  occurs at  $t = 0$  s. Then, at  $t = 3$  s, a frequency ramp of 50 mHz/s occurs for 2 s, followed by a steady-state frequency of 49.9 Hz until the end of the simulation. Since the focus of this paper is on the active power behavior of the control concepts, the voltage

TABLE I  
TRANSFER FUNCTIONS OF GRID-FORMING CONTROL CONCEPTS AND EVALUATION OF THEIR INSTANTANEOUS AND STATIONARY BEHAVIOR.

Grid-Forming Control Concept	Transfer Function $G(s) = \frac{\theta(s)}{\Delta p(s)}$	Instantaneous Behavior	Stationary Behavior
		$\lim_{t \rightarrow 0} \frac{1}{\Delta p(t)} \dot{\theta}(t)$	$\lim_{t \rightarrow \infty} \frac{1}{\Delta p(t)} \dot{\theta}(t)$
SE	$\frac{1}{s^2 T_a + s k_d}$	$T_a$	$\infty$
Droop	$\frac{m_p}{s^2 T_f + s}$	$\frac{T_f}{m_p}$	$\infty$
<i>Selfsync</i>	$\frac{m_p (s m_{pp} + 1)}{s^2 T_f + s}$	0	$\infty$
PSL	$\frac{k_p}{s}$	0	$\infty$
VSM0H	$\frac{D_f}{s} (1 + \frac{s k_D}{\tau_{k,D} s + 1})$	0	$\infty$
VCI	$\frac{K_{fp}}{s} + \frac{K_{fi}}{s^2}$	0	$\frac{1}{K_{fi}}$
DVC	Nonlinear Behavior	0	$\infty$
SEAF	$\frac{s T_w + 1}{s^2 T_a T_w + s k_d T_w}$	$T_a$	$k_d T_w$
SEFAD	$\frac{s k_{dd} + 1}{s^2 T_a + s k_d}$	0	$T_a$
SEDF	$\frac{s T_d + 1}{s^2 T_a T_d + s (T_a + k_d T_d)}$	$T_a$	$T_a + k_d T_d$
SG	$\frac{1}{s^2 T_a}$	$T_a$	$T_a$

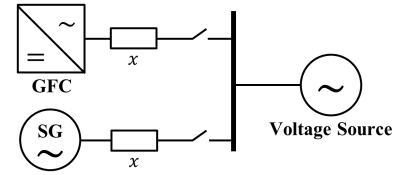


Fig. 3. Network model of the simulative comparisons.

amplitude setpoint of the stiff voltage source, as well as the converter setpoint voltage amplitude remain constant in all simulations. Based on the theoretical insights, the parameters of the grid-forming control concepts were chosen such that a well comparable dynamic behavior can be expected. The parameter values are listed in Table II. The simulation results are shown in Fig. 4. The simulation results with the control concepts of Section II are displayed in the left column of Fig. 4, while the simulation results of the control concepts of Section III are shown in the right column. The frequencies shown are the derivative of the phase angle. The frequency displayed of the SG is its rotor speed. At the beginning of each simulation, both the SG and the GFC do not feed in any active power.

At  $t = 0$  s, the phase angle jump of  $1^\circ$  causes a step change in the active power output of all feed-ins, which is inversely proportional to the reactance  $x$  and proportional to the angle difference. This active power output causes a short resynchronization, which can only be achieved by a temporary frequency deviation. The damping behavior of this transient process depends on the SG parameters and the parameters of the control concepts. While the SG cannot react to the phase angle jump with a step change of its rotor frequency due to its physical inertia, some of the GFC control concepts react to the phase angle jump with

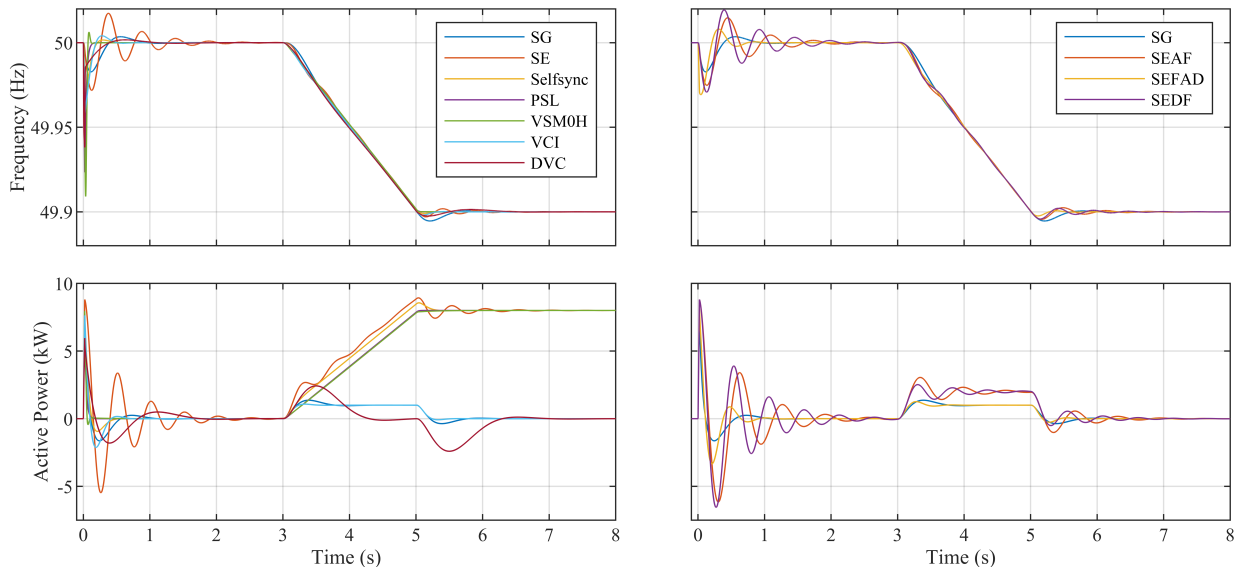


Fig. 4. Simulation results of the response to a phase angle jump of  $1^\circ$  at  $t = 0$  s and to a frequency ramp of 50 mHz/s from  $t = 3$  s until  $t = 5$  s. Left column: control concepts presented in Section II. Right column: modifications presented in Section III. Since the control concepts SE and droop are equivalent, only the simulation result of SE is shown. The basis of the comparison are the simulation results with a model of a SG.

TABLE II  
PARAMETERS OF THE SIMULATIVE COMPARISONS.

Grid-Forming Control Concept	Parameters (pu if no unit is specified)
Swing Equation	$T_a = 10$ s; $k_d = 40$
Droop	$T_f = 0.25$ s; $m_p = 0.025$
Selfsync	$T_f = 0.25$ s; $m_p = 0.025$ ; $m_{pp} = 5$
PSL	$k_p = 0.025$
VSM0H	$D_f = 0.025$ ; $k_D = 0.1$ ; $T_D = 250$ ms
VCI	$K_{fpp} = 0.01$ ; $K_{fi} = 0.1$
DVC	$R_d = 0$ ; $G = 1$ ; $J = 0.1$ ; $k_p = 5$ ; $k_i = 20$
SEAF	$T_a = 10$ s; $k_d = 200$ ; $T_f = 100$ ms
SEFAD	$T_a = 10$ s; $k_d = 0$ ; $k_{dd} = 25$
SEDF	$T_a = 10$ s; $k_d = 40$ ; $T_d = 250$ ms
SG	$T_a = 10$ s; $x_d = x_q = 1$ ; $x'_d = x'_q = 0.3$ ; $x''_d = x''_q = 0.1$ ; $T'_d = T'_q = 50$ ms; $T''_d = T''_q = 15$ ms

a step change of their frequency. The SE (and droop) as well as SEAF and SEDF behave analogously to the SG and also do not change their converter frequency in a stepwise fashion. All other concepts, on the other hand, respond with a step change in their converter frequency. This confirms the theoretical results obtained earlier, since these concepts do not limit the acceleration of the converter voltage phase angle after a step change in active power.

Each feed-in then responds to the frequency ramp by increasing its active power output. While the SG and the control concepts VCI, DVC, as well as SEAF, SEFAD and SEDF settle at a constant active power output during the frequency ramp, the output of the other control concepts continues to increase proportionally to the frequency deviation. This is again consistent with the theoretically obtained findings, since only these control concepts have finite stationary behavior after a step change in active power, i.e. they do not provide FCR.

## V. CONCLUSION AND OUTLOOK

GFC can mimic essential properties of SG and thus enable interconnected power system operation with 100% converter-based generation. However, suitable GFC control concepts do not have to copy the dynamic behavior of SG defined by its physics. After all, not every dynamic aspect of the SG makes sense from a stability point of view – limited inherent oscillation damping, requiring power system stabilizers for instance. As a number of GFC concepts have been developed in recent years, it is becoming increasingly difficult to keep track of them. Hence, this paper compares the most discussed control concepts by a system-theoretical analysis and by means of simulations, both with respect to their nominal behavior, i.e. without active limitations.

A closer look at the underlying system equations reveals similarities that are not obvious at first sight. Special attention is paid to the instantaneous and stationary behavior. While SG cannot change their speed in a stepwise fashion due to physics, many of the GFC control concepts presented are able to do so. If only a small number of GFC are equipped with such a control concept, a relevant influence on the grid frequency is not to be expected. This is probably no longer the case beyond a certain share of such GFC. Locally high frequency gradients and frequency deviations could be the result. As a possible consequence, certain loads based on synchronous machines could be harmed by such frequency gradients, or RoCoF-based protection systems could be falsely triggered. Against this background, it is necessary to investigate whether this instantaneous behavior in case of load steps is acceptable for the stability of all parts of the power system before a final specification of GFC.

## ACKNOWLEDGMENT

The presented work was financially supported by the German Federal Ministry for Economic Affairs and Energy

in the context of the research project “VerbundnetzStabil” (FKZ 0350015).

#### REFERENCES

- [1] P. Unruh, M. Nuschke, P. Strauß, and F. Welck, “Overview on Grid-Forming Inverter Control Methods,” *Energies*, vol. 13, no. 13, 2020.
- [2] U. Markovic, “Towards reliable operation of converter-dominated power systems: Dynamics, optimization and control,” Ph.D. dissertation, ETH Zurich, 2020.
- [3] A. Tayyebi, F. Dörfler, F. Kupzog, Z. Miletic, and W. Hribernik, “Grid-Forming Converters - Inevitability, Control Strategies and Challenges in Future Grids Application,” *CIREN Workshop - Ljubljana, 7-8 June 2018*, 2018.
- [4] ENTSO-E, “High Penetration of Power Electronic Interfaced Power Sources and the Potential Contribution of Grid Forming Converters: ENTSO-E Technical Group on High Penetration of Power Electronic Interfaced Power Sources,” 2020.
- [5] M. Kersic, T. Müller, E. Lewis, T. Schaupp, R. Denninger, P. Ernst, S. Reichert, S. Rogalla, R. Singer, A. Roscoe, K. Jalili, A. Dysko, A. Alvarez, Q. Hong, H. Lens, and C. Schöll, “Testing Characteristics of Grid Forming Converters Part 1: Specification and Definition of Behaviour,” *19th Wind Integration Workshop - Berlin, 11-12 November 2020*, 2020.
- [6] VDE FNN, “VDE FNN Hinweis: Spannungseinprägendes Verhalten von HGÜ-Systemen und nichtsynchrone Erzeugungsanlagen mit Gleichstromanbindung,” 2020.
- [7] V. Blasko and V. Kaura, “A new mathematical model and control of a three-phase AC-DC voltage source converter,” *IEEE Transactions on Power Electronics*, vol. 12, no. 1, pp. 116–123, 1997.
- [8] S. D’Arco and J. A. Suul, “Virtual synchronous machines — Classification of implementations and analysis of equivalence to droop controllers for microgrids,” *Power Tech - Grenoble 16-20 June 2013*, pp. 1–7, 2013.
- [9] —, “Equivalence of Virtual Synchronous Machines and Frequency-Droops for Converter-Based MicroGrids,” *IEEE Transactions on Smart Grid*, vol. 5, no. 1, pp. 394–395, 2014.
- [10] A. Engler, “Device for parallel operation of equal range single- phase or three- phase voltage sources,” Patent EP 1 286 444 B1, 2006.
- [11] L. Zhang, “Modeling and Control of VSC-HVDC Links Connected to Weak AC Systems,” Ph.D. Thesis, Royal Institute of Technology, School of Electrical Engineering, Stockholm, 2010.
- [12] M. Yu, A. J. Roscoe, C. D. Booth, A. Dysko, R. Ierna, J. Zhu, N. Grid, and H. Urdal, “Use of an inertia-less Virtual Synchronous Machine within future power networks with high penetrations of converters,” in *Power Systems Computation Conference 2016*.
- [13] S. Laudahn, J. Seidel, B. Engel, T. Bulo, and D. Premm, “Substitution of synchronous generator based instantaneous frequency control utilizing inverter-coupled DER,” in *2016 IEEE 7th International Symposium 27-30 June 2016*.
- [14] M. Ndreko, S. Rüberg, and W. Winter, “Grid Forming Control for Stable Power Systems with up to 100 % Inverter Based Generation: A Paradigm Scenario Using the IEEE 118-Bus System,” *17th Wind Integration Workshop, 17 - 19 October 2018*, 2018.
- [15] D. Duckwitz, F. Welck, and C. Glöckeler, “Betriebsverhalten der Virtuellen Synchronmaschine - Operational Behavior of the Virtual Synchronous Machine,” *Beiträge der 12. ETG/GMA-Tagung Netzregelung und Systemführung, 26.-27. September 2017 in Berlin*, 2017.
- [16] A. Dysko, A. Egea, Q. Hong, A. Khan, P. Ernst, R. Singer, and A. Roscoe, “Testing Characteristics of Grid Forming Converters Part 3: Inertial Behaviour,” *19th Wind Integration Workshop - Berlin, 11-12 November 2020*, 2020.